RESEARCH ARTICLE

Power Reversal Algorithm for Resonant Direct Current Transformers for DC Networks

RENAN PILLON BARCELOS[1], **(Graduate Student Member, IEEE),**
JAKUB KUCKA[1,2]**, (Member, IEEE), AND DRAZEN DUJIC**[1]**, (Senior Member, IEEE)**
[1]Power Electronics Laboratory, École Polytechnique Fédérale de Lausanne (EPFL), 1015 Lausanne, Switzerland
[2]Siemens AG, Large Drives Applications, 91058 Erlangen, Germany

Corresponding author: Renan Pillon Barcelos (renan.pillonbarcelos@epfl.ch)

ABSTRACT The bidirectional resonant DC transformer has all the desired features to drive the development of the DC power distribution networks of the future. This power-electronics converter provides galvanic isolation between DC buses, has desired open loop properties, and follows the system's power flow naturally, requiring only a power reversal algorithm to allow a bidirectional operation and smooth transitions. This paper proposes a solution to tackle the power reversal of the DCT with a dynamic algorithm, considering the system behaviour and the power converter characteristics. The proposed algorithm executes the power reversal in few switching periods and removes the DCT losses during no-load condition. Then, using low voltage prototype of DC transformer, experimental results along the paper demonstrate how this power reversal algorithm is applied under various operating conditions.

INDEX TERMS LLC converter, DC transformer, DCT, resonant converter, power reversal, power transition.

I. INTRODUCTION

The medium voltage DC power distribution network (PDN) have been proposed to grid operators as an alternative to expand their infrastructure and handle the increasing volumes of distributed and renewable energy sources. Some applications as electric ship PDNs, photovoltaic and wind plants collection grids, and data centers, have already found great benefits from DC PDN as its main architecture [1], [2], [3]. However, a few milestones are yet to be reached in order to make the MVDC PDN preferable to the MVAC solution.

One of the challenges is the development of high-power and medium-voltage DC-DC converters to interface two DC buses. This power converter has its crucial importance to realize flexible DC grids, allowing the voltage adaptation and interconnection between two different DC buses. This paper addresses this converter as DC Transformer (DCT), relating its functionality to the well-know AC transformer. An equipment allowing for the voltage adaptation, and adjusting the power flow naturally. Figure 1 shows an example of a DC

The associate editor coordinating the review of this manuscript and approving it for publication was Md. Mejbaul Haque
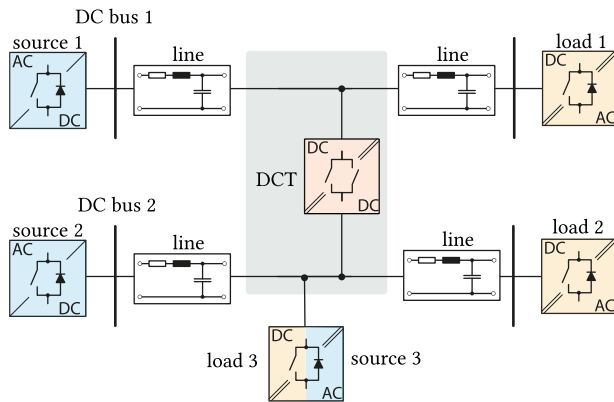
PDN with 6 nodes, and one DCT. Ultimately, the goal of the DCT is purely to connect the DC buses providing the power exchange when the power flow changes, and galvanic isolation.

In this sense, the main desired characteristics of a DCT are:

- High efficiency, simplicity, robustness, and no closed-loop control;
- Load independent behavior, bidirectional, and isolation at high frequency.

In literature, one type of solution are the converters based on dual active bridge topology [4], [5], the closed-loop controlled resonant converters [6], [7], and multilevel converters [8], [9], often addressed as DCX converters [10], [11], [12]. These solutions are able to perform high efficient DC-DC conversion, isolation, and bidirectional operation: However, they operate based on a closed-loop control that would require some strategy to issue the set-point, which can be given by the grid operator or by some droop based control. In this way, the DC-DC converter will not be driven by the natural power flow of the DC grid, which will impact the complete system's dynamic and stability [13], [14], [15]. Consequently, different

FIGURE 1. DC power distribution network with 2 DC buses, and one DCT. In this system, load dynamics can change the power flow, and thus; DCT should enable the power exchange every time it is requested. In the shaded area the scope of the work.

solutions might be preferable to realize a DCT to fulfill the desired characteristics.

A different solution is to use the resonant LLC converter operating near the switching frequency. This converter provides a stiff voltage-ratio loading characteristics. Yet, the power stages connected on each DC port can operate individually, and do not require any synchronization or signal feedback between them. Hence, when one side is switching, the other side can operate as a passive rectifier, requiring only one PWM reference for the DCT; and when the power flow reverses, the power stages alternate their responsibilities and redirect the current to the other side. This feature is very welcome for DCTs, especially for DCTs using bipolar devices (e.g. IGBTs) where the active rectification increases the switching losses and thus reduce the overall efficiency.

Nevertheless, to allow bidirectional operation, the resonant converter requires a certain minimum of intelligence to identify where to direct the power. In literature, some papers present solutions using the voltage gain of the converter with voltage measurements to decide about the power direction [6], [16]. This solution requires on a good voltage measurement and complete knowledge of the DCT and the system under analysis. For instance, in [6] a hysteresis voltage band is used to detect the power flow direction of the converter. In that case, the power direction changes when the output voltage hits the borderlines of the hysteresis voltage band.

Other way to address the power reversal question is by keeping both power stages actively switching [12], [17], [18], [19], [20]. These solutions can ensure higher quality of the power transition dynamics, however they require a relatively precise knowledge of the converter circuit since both converter sides are operated concurrently.

In our previous proposed solution available in [21], the resonant currents are used to determine when to reverse power. The active bridge switchover (ABS) method is based on observing the peak current at the resonant current and

identifying the eminent power reversal. However, a few issues were not addressed in that strategy, namely:

- Start of DCT: As the method relies on the resonant current measurements, the correct direction during the initialization of the DCT is uncertain. Thus, the DCT needs to start with one direction, and if it is wrong change to the other.
- Jittering around zero: During power reversal - specially slow power reversal - the method computes several power transitions, unnecessary transitions where any power is really transferred.

Therefore this paper addresses these two main question. First, the start of DCT is tackled by using the dc voltage measurements that are always available on its terminals. Further, by using only dc voltages the power direction is computed, and the dynamic of the voltages (indirectly power dynamic) are used to determine duration of soft-start. Second, a new operation mode is introduced to deal with jittering and to remove the operational losses of DCT when operating in no-load condition. This approach leads to a more complete open loop strategy for the DCT operation.

The next section will describe the DCT topology, and the DC power distribution network into analysis. Then, in Section III, the power reversal strategy will be explained along with the description of the soft-start, Idle Mode, Power Reversal Method and the combination of all these strategies to create the Power Reversal Algorithm addressed in this paper. In Section IV, the final experiments are demonstrated and in Section V, the conclusion of the work are summarized.

II. DCT TOPOLOGY AND DC PDN

The DC PDN under analysis is shown in Fig. 1. In this system the DCT is connected to two different DC buses, where the voltages of the nodes 1 and 2 are regulated by converters 1 and 2, respectively. The DCT's goal is to interface the two buses allowing the power flow throughout its branch, and not creating nor regulating DC bus. In this sense, the DCT only observes the voltages on its terminals, and is not aware of the complete system.

Depending on the loads' dynamics and extra elements of the DC PDN, the voltages at the DCT's ports change according to the system's power flow. An simple example is to imagine that Load 1 is disconnected, resulting in less current flowing through DC bus 1 and increasing the voltage of DCT's port. Another example is if the Load 3 stops consuming and turns into a Source 3, it will increase the voltage and modify completely the power flow. Among other situations that could happen, the focus of this paper is to develop an algorithm to perform the power reversal, which is also robust against DC PDN transients (e.g. load disconnections, DC voltage oscillation, etc.)

The resonant DC transformer under analysis is shown in Fig. 2. The DCT is constructed as a symmetric LLC with split capacitors around the Medium Frequency Transformer (MFT). The design guidelines of such converter can be found in [6], [23], and [24]. The power stages of each DC port can be
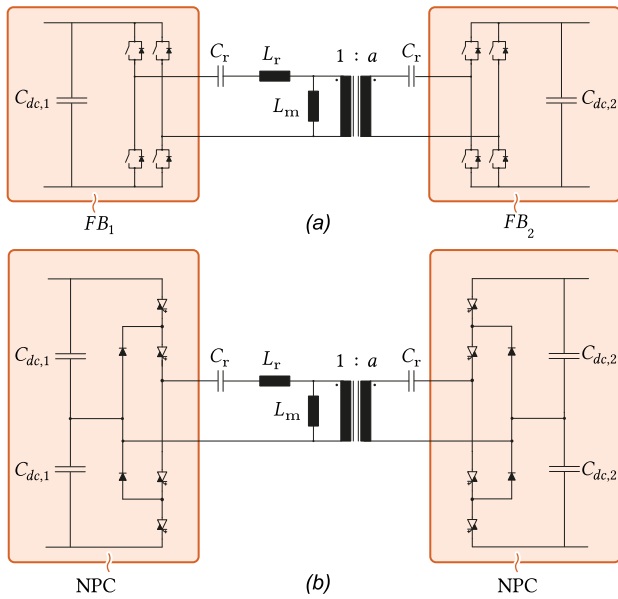
FIGURE 2. DCT with different power stages; (a) Full-bridge used for experimental investigation presented in the paper; and (b) NPC suitable for MV MW applications [22].

FIGURE 3. Simplified schematic of the DCT, from Fig. 14. Parameters and ratings are available in Table 1. Details on voltages and current measurement points correspond to presented experimental waveform.

FIGURE 4. Finite-state machine of ABS strategy from [21].

FIGURE 5. Illustration of the idle Mode operation principle. The DCT initialized only when the ΔV_{DCT} overcomes ΔV_{DCT}^{th}, with slow soft-start. In case the voltage variation is too aggressive, the soft-start period is reduced. At the moment the power being processed by DCT is below a P_{th}, the DCT stop switching, improving the efficiency. V_{ab} is the output voltage of power stages applied to the resonant tank.
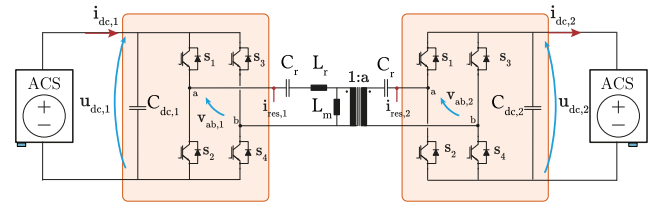
any topology capable of creating at least three level voltage in the resonant tank. In Figure 2, two DCTs are shown, using full bridge modules and Neutral Point Clamped (NPC) leg with split capacitors. The DCTs with full-bridge modules with unipolar PWM have the ability to perform all the aforementioned requirements for a DCT (i.e. bidirectional operation and three-level operation).

In this paper FBs power stages are used to test the methods due to accessibility of LV equipment, sufficient to demonstrate the power reversal methods performances. However, presented algorithm is developed for MV prototype where IGCT NPC leg in combination with split capacitor bank [22], [25]. Results are not affected by the topology once the only aspect that matters are the square wave generation on the ac side, capacity to create three-level for the transient, and bidirectionally.
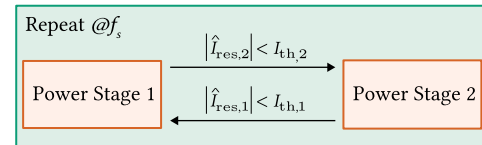
III. DESCRIPTION OF THE POWER REVERSAL ALGORITHM

In this section each part of the Power Reversal Algorithm (PRA) is described, along with experimental demonstration of the specific section. The test setup and its power ratings are presented later in Section IV. Nevertheless, in order to anticipate experimental results, Figure 3 shows a simplified schematic of the system, with the considered references for the measurements. The two DC sources create the dc buses, and the DCT transmit the power according to the dc voltages.
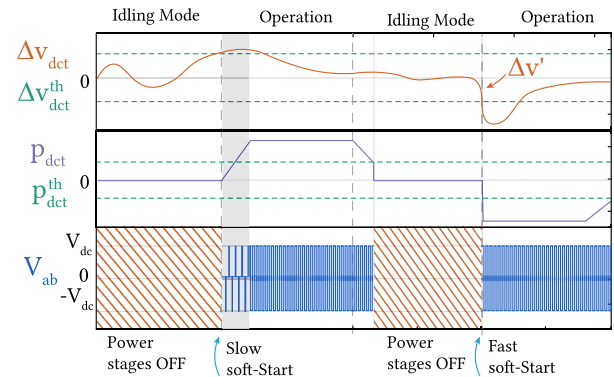
In our original solution [21], the ABS is based on observing the peak current at the resonant current. This method rely on monitoring the resonant current and deciding which power

stage should be actively switching. Fig 4 shows the finite machine of this method.

However, as already mentioned, this method is not capable of identifying the power direction when there is no current in the DCT. What ABS does is to alternate the power stages until the power flow is well defined to one side.

In this case, at the moment the DCT is OFF (idle), the only variables available to predict the power direction are the DC voltages. Therefore, this is the only way to initialize the DCT correctly, rather than randomly. Taking this as an advantage, the idle state of the DCT can be used to set the operation limit of the DCT, creating a operation mode called Idle Mode (IdM). In this case, not only the DCT will initialized with the correct power direction when enabled, but it will start its operation only when enough power is expected to be transferred, avoiding unnecessary losses due to the magnetizing current of MFT.
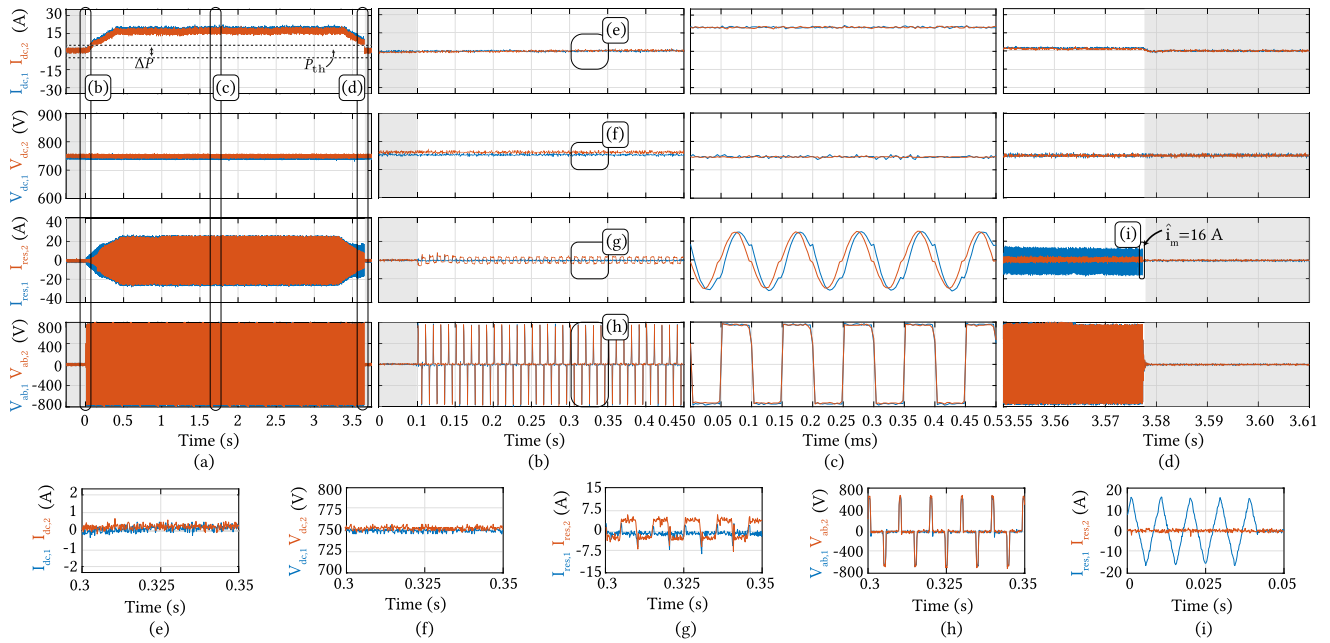
FIGURE 6. Experimental waveforms showing the DCT in Idle Mode, with a power threshold. In (a) overview of the Idle mode operation; in (b) details on the soft-start; in (c) the operation waveforms; and in (d) details on the turn off moment. During the shaded period, DCT is in idle state waiting for the expected power to overcome its threshold. At $t = 0$ s the DCT turns on by noticing the DC voltages mismatch. Then, once the DC buses returns to equilibrium after $t = 3.5$ s, the DCT turns off, as the power is below the threshold value. In (e), (f), (g), and (h) zoom-in on the soft-start waveforms; (e) details on the dc current (f) details on the dc voltages; (g) details on the resonant currents, and (h) details on the three level voltage applied to the resonant tank. In (i) zoom-in on the resonant current when DCT is processing only magnetizing current.

Therefore, this operation mode is integrated to the soft-start strategy and power reversal detection to enhance the power reversal algorithm.

A. IDLE MODE

Essentially, this mode defines when the DCT should turn ON and turn OFF. Fig. 5 illustrates the Idle Mode operation principle. In this figure is possible to see that, as soon as the voltage difference between the primary and secondary side, $(\Delta V_{dct} = V_{dc,1} - V_{dc,2})$, are different and above a certain hysteresis band, the DCT starts transmitting power. Then, DCT stays in the active operation mode until the power being processed contains only the no-load losses of converter. At that moment, the DCT enters in idle mode, and stays idle until the voltages difference overcome the pre-defined threshold again.

In Figure 6, the experimental demonstration of this operation mode is shown. At the first moment, the two buses are in equilibrium, and no power is transferred. Then at $t = 0$ s, the DCT detected the $\Delta V_{dct} > \Delta V_{dct}^{th}$ (which in this example is $\Delta V_{dct}^{th} = 3$ V), and the DCT starts its operation. After $t = 3.3$ s the DC buses return to equilibrium. At that moment, the DCT stop switching to reduce losses, when there is no need for DCT to transfer any power. In this experiment the power threshold was set to $P_{dct}^{th} = 1$ kW.

Different variables could be used to identify that only losses are present in the DCT. For instance, the threshold could also be set by observing both resonant currents and verifying if only magnetizing current is existing. In any case,
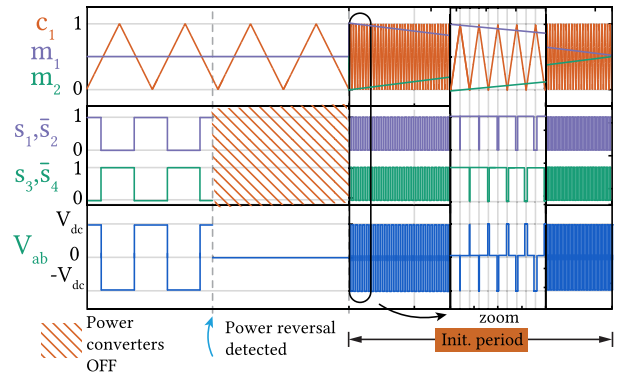

FIGURE 7. Illustration of the PWM initialization sequence, and zoom in the three-level voltage in the resonant tank after power reversal. c_1 is PWM carrier, m_1 and m_2 are modulation index for leg 1 and leg 2 respectively. s_x is the gate signal of device x, and V_{ab} is resonant tank voltage. After power reversal detection, DCT is in IdM for two switching periods, and starts the initialization sequence with soft-start.

it is worth mentioning that both threshold values are set according to the the parameters of the DCT.

Thus, the no-load losses can be avoided if DCT intelligence turns-off DCT and enters in Idle Mode. For the case of the prototype used in this paper, the no-load losses represents 0.45% of nominal power (100kW) [26], [27], [28].

B. SOFT START

As it is well known and demonstrated in the literature, saturation of MFT and large inrush currents should be avoided. There are many methods already available [6], [29],
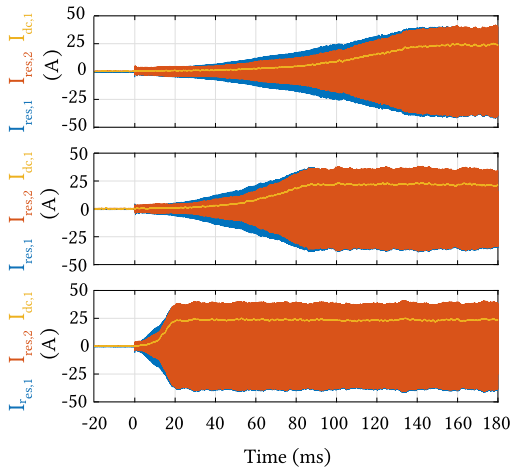
FIGURE 8. Experimental waveforms showing the soft-start of From the top to the bottom, the soft-start duration is: 0.14 s, 0.08 s and 0.014 s.
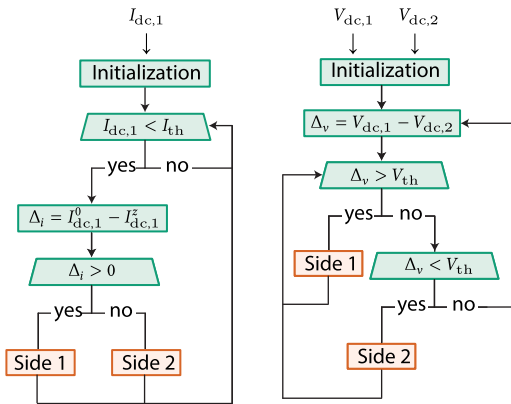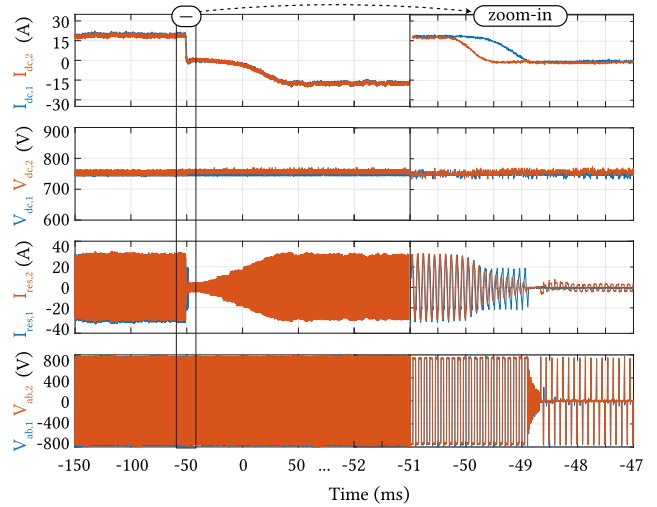

FIGURE 9. Power direction identification with a threshold band to avoid jittering. In (a) the PRM-1, based on the DC current rate of change; (b) PRM-2, based on the DC voltages; All the PRMs run indefinitely with DCT's operation. Side 1 or 2 refers to power stage 1 or 2, relating to the DC port.

FIGURE 10. Experimental waveforms showing the response of the DCT for the step reverse ($dv/dt = 5 \ V/\mu s$), using the PRM-1, based in the rate of change of the DC currents. Zoom shows the moment of the power reversal, where it is possible to note that DCT enters in IdM and starts its initialization sequence with a three-level waveform. Before the method detect the power reversal, the DCT stays during a period of time with only the magnetizing current noticeable in the third plot in blue. During the IdM, a resonance to equalize the voltages over switches occur in the resonant tank.
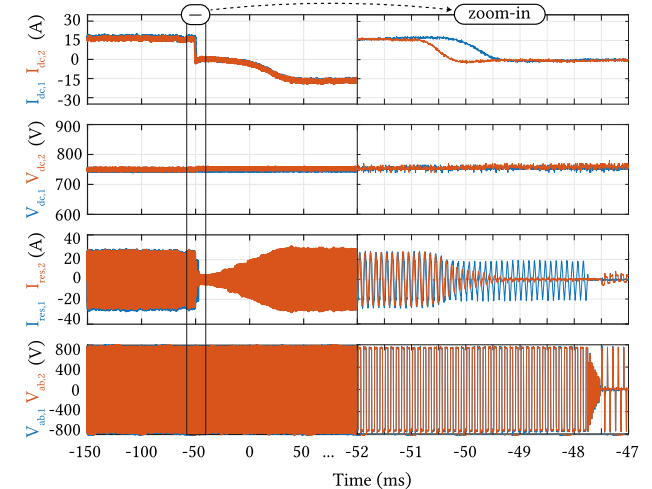
FIGURE 11. Experimental waveforms showing the response of the DCT for the step reverse ($dv/dt = 5 \ V/\mu s$), using the PRM-2, based in DC voltages. Direction of the currents correspond to the schematic of the system. Zoom shows the moment of the power reversal, where it is possible to note that DCT enters in IdM and starts its initialization sequence with a three-level waveform.

[30], [31], and this paper adopts the duty cycle modulation, applied during every DCT start.

This strategy is illustrated in Fig. 7. At first, the power stage is switching with both modulation indices being 0.5. Then, at certain point the DCT went OFF and at the moment to start its operation again, the modulation indices were set accordingly to apply a three-level waveform to the resonant tank.

During this period the DCT operates in a strongly non-linear and partly discontinuous behavior until it reaches the 50% duty cycle. For that reason, one important feature of the soft-strategy for DCTs is the ability to adaptively change the soft-start time duration accordingly to the power demand.

Thus, by using the only two available variables (DC voltages), the speed of the soft-start can be determined by the rate of change of the voltage ($\Delta V'_{DCT}$.) If this value is high

the soft-start will be fast (short) and if it is low the soft-start will be slow (longer).

To demonstrate the different dynamics for different soft-start speed, Fig. 8 shows an experimental results for the soft-start with three different speeds. The considered cases consist in: i) Fast soft-start ($140 T_{sw}$), when the rate of change of the voltage is $\Delta V' > 0.1$ V/μs; ii) Medium speed ($800 T_{sw}$), when the rate of change of the voltage is between
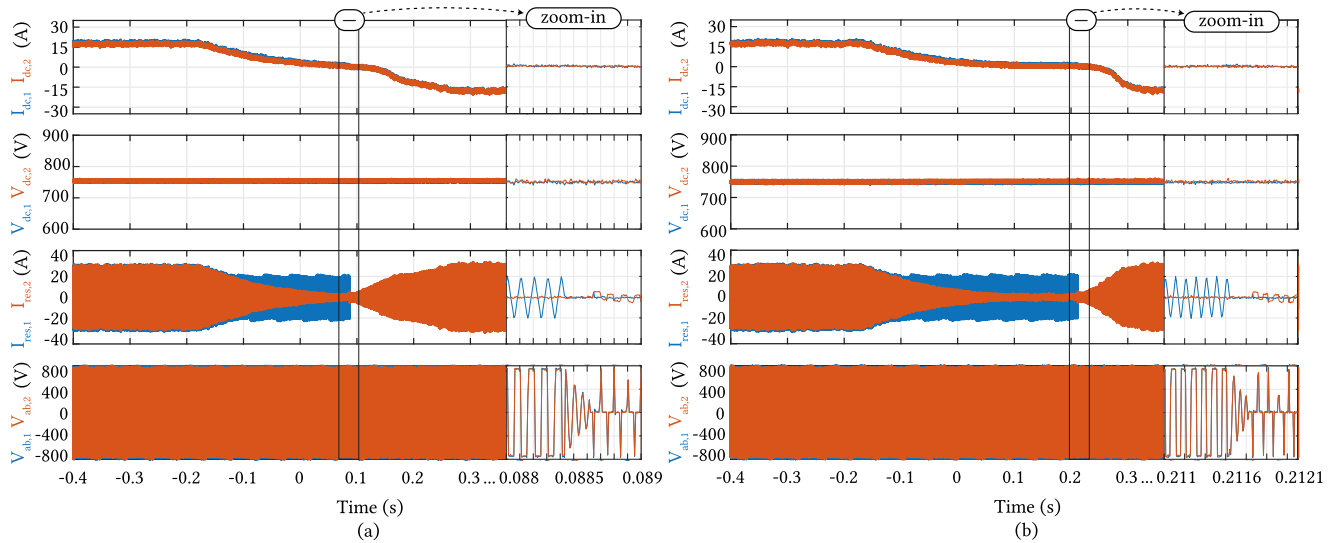
FIGURE 12. Experimental waveforms showing the response of the DCT for the slow reverse (SR), using the (a) PRM-1, based in the rate of change of the DC currents, and (b) PRM-2, based in DC voltages. Zoom shows the moment of the power reversal, where it is possible to note that DCT enters in IdM and starts its initialization sequence with a three-level waveform. It is noticeable from third plot that the PRM-2 detected the power reversal later.

$0.01 < \Delta V' < 0.1$; iii) Slow soft-start of $(1400T_{sw})$, when the rate of change of the voltage is $\Delta V' < 0.01$ V/μs.

Thus, the duration of the soft-start becomes a parameter for the Power Reversal Algorithm, where depending on the load dynamics, the initialization of the DCT is set accordingly.

C. POWER DIRECTION IDENTIFICATION

The power direction identification is performed by the open loop strategies that determines which power stage should be active to follow the natural power flow. One strategy already mentioned is the ABS [21], with its finite-machine described in Fig. 4. This strategy could be used after the initialization of the DCT to identify the power direction, with small adaptation on the IdM to avoid jittering.

In this paper, other two different strategies are described and tested. Fig. 9 describes both strategies; One using the DC current derivative, and the other using DC voltages. The first method is called PRM-1 (power reversal method - 1). It determines the necessity for the power reversal from the DC current variation. This method can be a lead indicator, where the method commands the power reversal when the current is within the threshold band. Essentially, this method is monitoring the sign of the rate of change of DC current (di/dt), and in low range of values of current, it triggers the power reversal if the derivative is leading to the opposite direction than the current signal. Thus, this method can anticipate the power reversal, and this can be beneficial for the very fast transition dynamics.

The second method described in Fig. 9 is based in the DC voltages (PRM-2). This PRM determines the power flow direction by acknowledging which DC port is higher/lower than the other.

Figures 10, 11, and 12 show the performance of these two PRMs for a load step change and load ramp change. In order
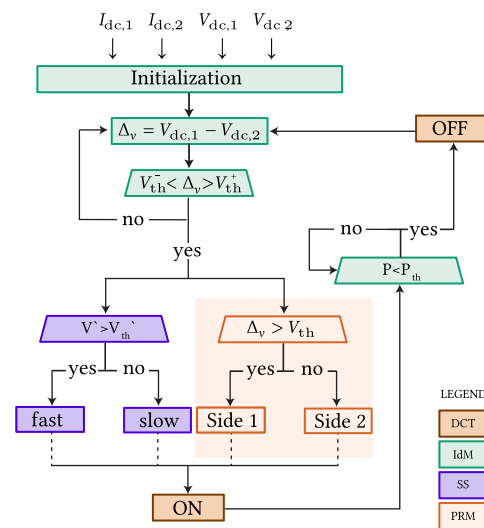

FIGURE 13. Power Reversal Algorithm, with PRM strategy based on the DC voltages. Each color correspond to a different section of the operation strategy.

to properly evaluate these two PRMs, the idle mode period was set to a fix period. It means, that once DCT enters IdM, the soft-start starts after a fixed amount of time (in this example $t_{idle} = 2 \times T_{sw}$.)

In Fig. 10 and 11 the load step is performed, changing $V_{DC,2} = 740$ V to $V_{DC,2} = 755$ V. The slope of the step change is $dv/dt = 5$ V/μs. In these figures it is possible to see that both methods had similar performance as expected, because the voltage variation is quite fast.

Now, in Fig. 12 the ramp load was performed, changing the $V_{DC,2} = 740$ V to $V_{DC,2} = 755$ V, with slope of $dv/dt = 0.025$ V/ms. In this figure it possible to see the
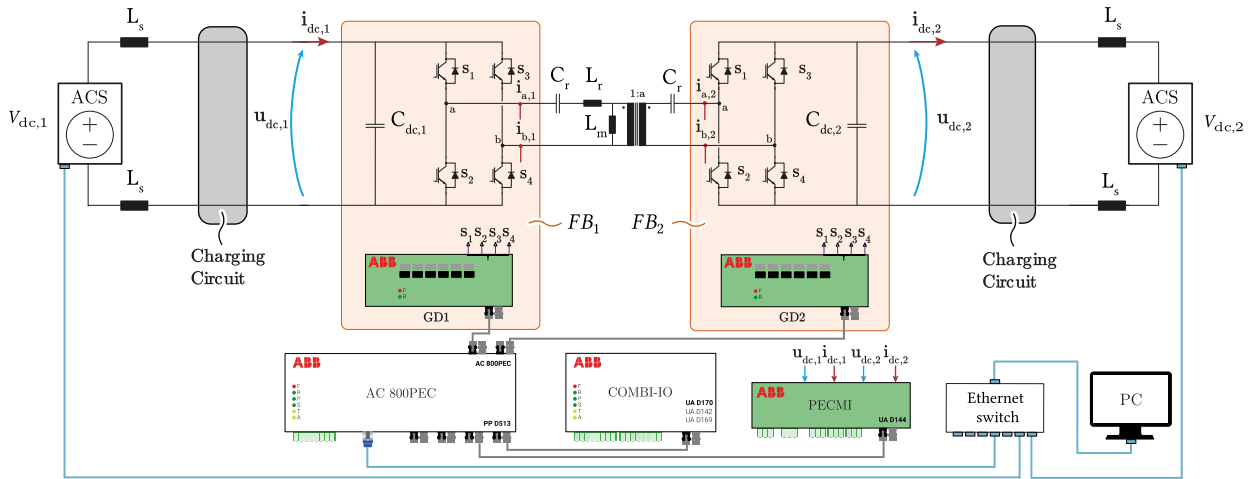
FIGURE 14. Schematic of the complete system. The two DC buses are created with voltage sources. Detailed measurements correspond to the actual measurements for the PRMs. For the test setup system, controller, relays, and power sources are accessed through PC.
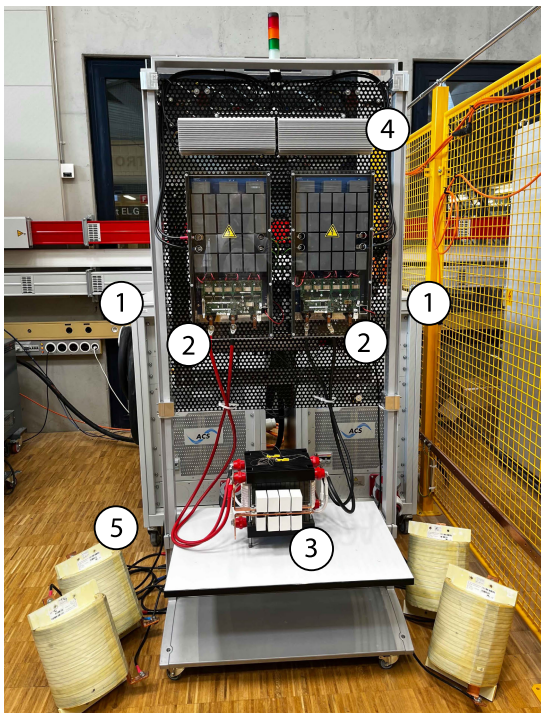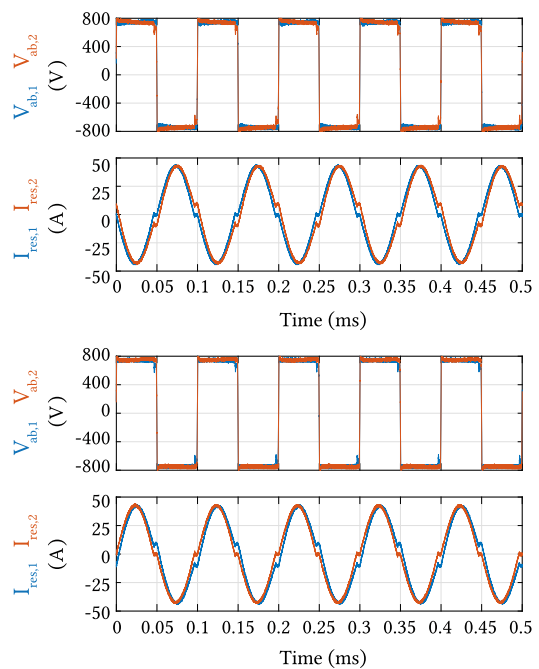

FIGURE 15. Photo of the DCT prototype in. 1 - ACS: DC buses; 2 - Power stages; 3 - MFT; 4 - Charging resisors, 5 - Grid inductor (L_S).

FIGURE 16. Experimental waveforms of forward and backward operation of DCT. Sub-resonant operation and turn-off current of $I_{m,off}$ = 16 A.

difference of each method. For the PRM-2, which is based on voltage measurement, the power reversal was detected after the PRM-1 had already set the power reversal based in the rate of change of the DC current. Either way, both methods were able to correctly predict the power reversal, and follow the logic of soft-start and Idle mode.

D. POWER REVERSAL ALGORITHM

In summary, the IdM strategy determines when the DCT should be activated, the SS determines how fast the power

transition should be according to the load dynamic, and lastly, the PRM determines the active power stage of the DCT.

Figure 13 shows the complete scheme for Power Reversal Algorithm (PRA). In this schematic, the required variables are the two DC voltages, indispensable for the DCT initialization, and at least one current in order to compute the power. Nevertheless, variations of this schematic can be created according to the available measurements.

With this algorithm, the DCT has a well defined open loop operation. The DCT starts operating when the voltage difference reach certain level, with a soft-start weighed with
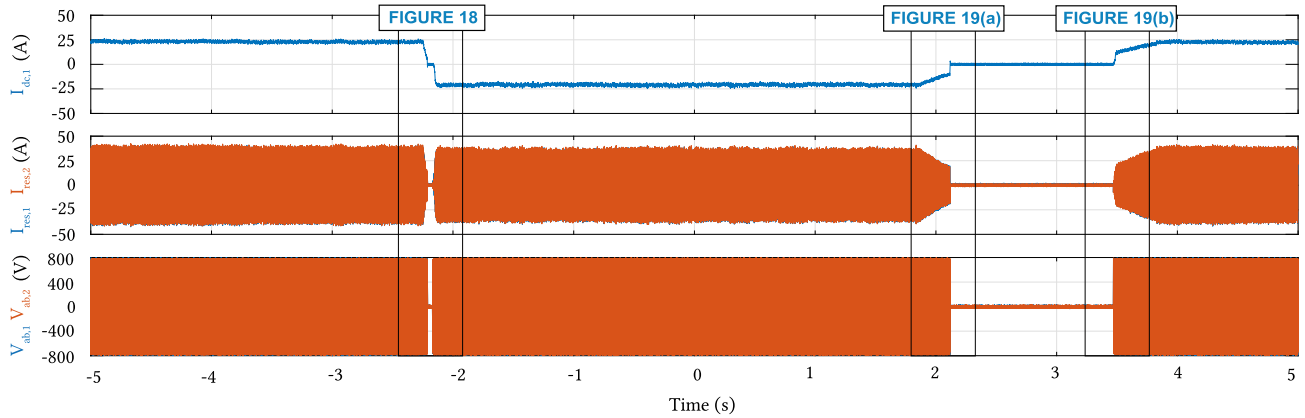
FIGURE 17. Experimental waveforms showing the response of the DCT for a fast power reverse, and slow power reversal. The DCT uses PRA to determine its operation limits and set the proper initialization time. Direction of the currents correspond to the schematic of the system. The DCT process power in both directions and a load profile is performed to test and validate the PRA. Squares mark the zoom available in Figures 18 and 19.

TABLE 1. DCT and system parameter.

Rated Voltage bus 1	$V_{DC,1}$	750 V
Rated Voltage bus 2	$V_{DC,2}$	750 V
Grid inductance	L_s	30 μH
Transformer Ratio	$1 : a$	1:1
Resonant Inductance	L_r	5.8 μH
Magnetizing Inductance	L_m	750 μH
Resonant Capacitance	C_r	37.5 μF
DC-link Capacitance	C_{DC}	1020 μF
Switching Frequency	f_s	10 kHz

the load dynamics, always to the correct direction. And then, goes OFF only when the processed power is below a defined power threshold. In this sense, the PRA is a robust strategy because in case of voltage spike or big transients in the voltage, the PRA will not issue any command, while the power stays above the minimum limit.

Besides that, the PRA brings the IdM operation that avoid unnecessary power consumption with magnetizing current, and eliminates any jittering around zero for fast and slow load dynamics.

IV. EXPERIMENTAL VALIDATION

In this section, the experimental setup used to gather all previously presented intermediate results is presented. The DCT is using a three-phase VSI developed in the lab, with only two legs operated as FB. The resonant tank consists of a 100 kW MFT with integrated resonant capacitors developed in [27]. The DC buses are created with two switched power amplifier - TC.ACS from Regatron, where two legs of 3-phase 50 kW were used, reducing the DC power ratings available for the experiments. The DCT is controlled by the ABB's AC 800PEC, and the schematic and experimental prototype are shown in Fig. 14 and Fig. 15, respectively. Table 1 shows the parameters of the system.

The design of the DCT follows the same procedure of the LLC converter. The design of the magnetizing inductance is

related to the desired turn-off current of power switches. The choice of the leakage inductance is usually guided by the desired quality factor. Then, the choice of the resonant capacitor is related to the desired resonant frequency in relation to switching frequency. More details can be found in [7], [21], [23], and [31].

The experimental setup consists in two energized DC buses from ACS, and the DCT with the charging resistors proceed with the start-up sequence. First the capacitors of DCT are charged through charging resistors which are further bypassed. Then, the DCT is enabled and PRA starts operating. Now, to simulate any load variation, the voltages of the two DC buses are modulated in order to provoke various power flows.

For all the experiments, the DC bus 1 was regulated to $V_{DC,1} = 750$ V, while the DC bus 2 varies following the emulated load dynamic. Therefore, in order to provoke a power flow around $P_{DC} \approx 20$ kW, the DC bus 2 is set to $V_{DC,2} = 742$ V. Figure 16 shows the experimental results for the resonant currents and voltages. On top the forward operation and on the bottom the backward operation. It can be notice that the turn-off current of DCT is around 16 A, and the converter is operating below the resonant frequency.

Now, Figures 17, 18, and 19 show the DCT operation with PRA. In Fig. 17, the complete operation with the step load and ramp load variation is shown. This figure make each function of the PRA clear. Firstly, the DCT is operating processing 18 kW, when suddenly, the power reverses when $V_{DC,2}$ increases from $V_{DC,2} = 744 \rightarrow 760$ V, with a slope of ($dv/dt = 5$ $V/\mu s$). The PRA, quickly identifies that the power was reduced and put DCT in idle, when the minimum power was reached (here set to $P_{th} = 3$kW for the purpose of demonstration); then, by noticing that the power direction changed, and that the variation of the voltage is higher then the $\Delta V'_{th}$, (here set to $\Delta V'_{th} = 0.01$ $V/\mu s$), the PRA triggered the fast initialization of the DCT, for the power stage 2.
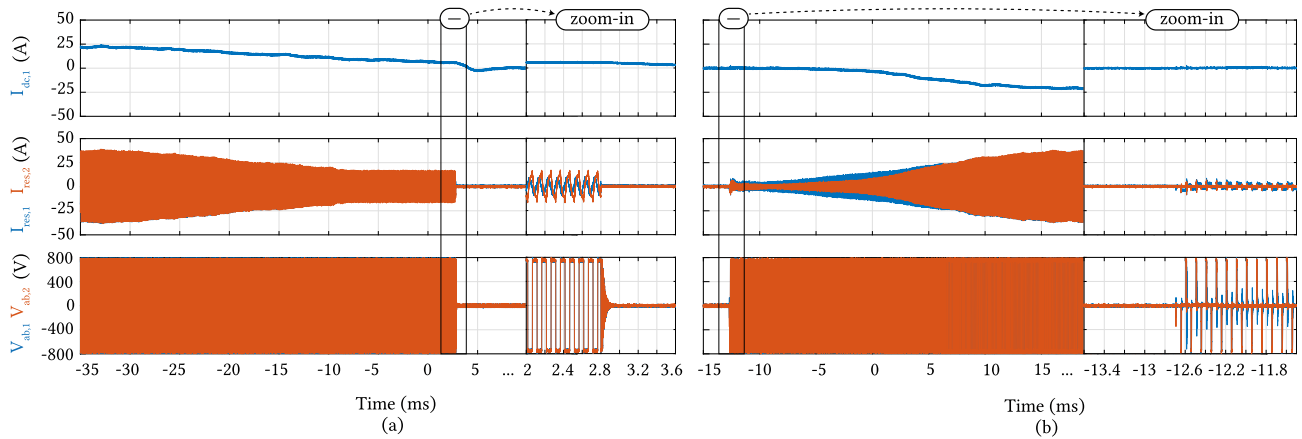
FIGURE 18. Experimental waveforms showing the response of the DCT for the fast power reversal (Zoom-in in the first transition of Fig. 17.) In (a) the moment DCT enters in Idle Mode by reducing the processed power below the threshold. Zoom-in in the moment DCT goes idle. In (b) the moment DCT starts the soft-start with fast dynamic load. Zoom-in the in the moment the power stage start switching.
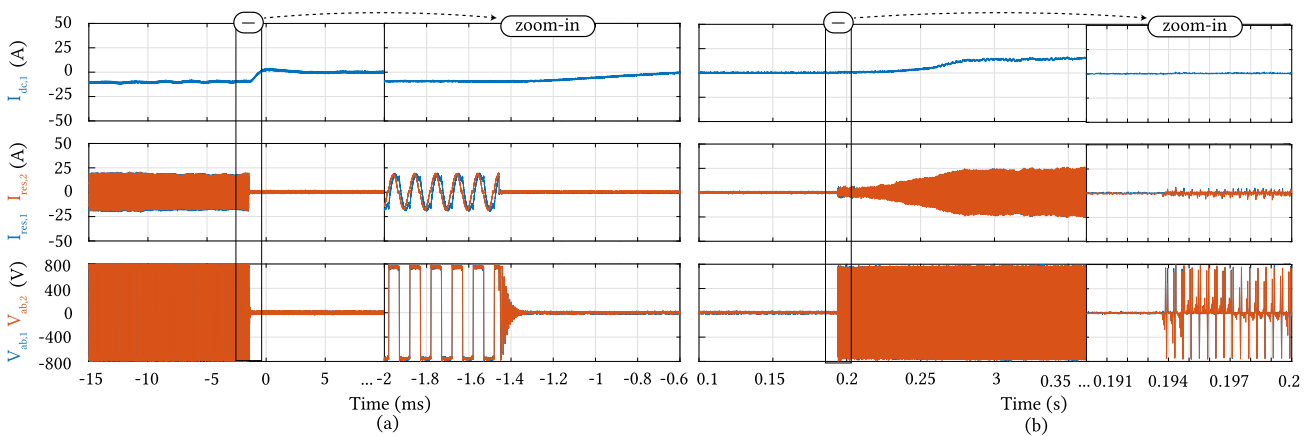
FIGURE 19. Experimental waveforms showing the response of the DCT for the slow power reversal (Zoom-in in the second and third transition of Fig. 17.) In (a) the moment DCT enters in Idle Mode by reducing the processed power below the threshold. Zoom-in in the moment DCT goes idle. In (b) the moment DCT starts the soft-start with slow dynamic load. Zoom-in the in the moment the power stage start switching.

The details of the first transition can be seen in Figure 18. Fig. 18(a) shows the details in the transition from the operation mode to the Idle mode; and in Fig. 18(b), the details of the soft-start initialization with a fast initialization time of $t_{ss} = 14$ ms.

Now, after a while the load changes again and start decreasing the $V_{DC,2}$ voltage slowly. At this moment, as soon as the power reduces and reach the power threshold, the DCT enters to the Idle Mode. Then, the $V_{DC,2}$ voltage keeps decreasing until the voltage difference between the two DC ports is bigger than the voltage threshold Δ_v^{th} (here set to $\Delta_v^{th} = 3$V.)

Thus, Fig. 19 shows details on the dynamics of this transition. Firstly, in Fig. 19(a) the DCT enters the Idle Mode at the moment the processing power is below the threshold. Then, in Figure Fig. 19(b) the soft-start of the power stage 1 of the DCT with a initialization time of $t_{ss} = 0.14$ s, as the load variation is slow.

In the end, the PRA performed well and as expected, following naturally the power flow given by the DC buses.

All the threshold values used in the paper were set with the knowledge of the DCT's parameters. For that, the dependence of the voltage gain on the power transferred curve of LLC was be used.

V. CONCLUSION

This paper proposed and demonstrated a power reversal algorithm for the DCT combining available voltages and current, and load dynamics. The presented algorithm contains essential features for the operation of the DCT including power reversal strategy, and idle mode operation. This approach led to a more complete open loop strategy to set the operation limits and allow bidirectionally of the DCT.

As demonstrated with experimental results along the paper, the operation of DCT with these features is very similar to the ac transformers. What makes the DCT operate with the desired characteristics to enable the future dc grids. Nevertheless, extra challenges could be found when the DCT operates with an MVDC grid.

The use of the Idle Mode to set the DCT operation limits was demonstrated and the main advantages are: correct and smooth initialization, no jittering in power reversal, and reduce losses in no-load conditions. This mode simplifies the control strategies of the DCT and let it operates according to the natural power flow, which is very beneficial for the DCT.

Finally, the operation of the DCT, as any open-loop control, requires some pre-set thresholds, based on the parameters of the DCT. Similarly, this paper relies on these values to define its operation limits; however, using the available models in the literature these values can be well determine, and fine-tuned with experimental characterization.

REFERENCES

[1] U. Javaid, D. Dujic, and W. van der Merwe, "MVDC marine electrical distribution: Are we ready?" in *Proc. 41st Annu. Conf. IEEE Ind. Electron. Soc. (IECON)*, Nov. 2015, pp. 000823–000828.

[2] S. Ullah, A. M. A. Haidar, and H. Zen, "Assessment of technical and financial benefits of AC and DC microgrids based on solar photovoltaic," *Electr. Eng.*, vol. 102, no. 3, pp. 1297–1310, Sep. 2020, doi: 10.1007/s00202-020-00950-7.

[3] K. Kim, K. Park, G. Roh, and K. Chun, "DC-grid system for ships: A study of benefits and technical considerations," *J. Int. Maritime Saf., Environ. Affairs, Shipping*, vol. 2, no. 1, pp. 1–12, Nov. 2018.

[4] R. W. De Donker, D. M. Divan, and M. H. Kheraluwala, "A three-phase soft-switched high-power-density DC/DC converter for high-power applications," *IEEE Trans. Ind. Appl.*, vol. 27, no. 1, pp. 63–73, Jan./Feb. 1991.

[5] X. Li and A. K. S. Bhat, "Analysis and design of high-frequency isolated dual-bridge series resonant DC/DC converter," *IEEE Trans. Power Electron.*, vol. 25, no. 4, pp. 850–862, Apr. 2010.

[6] J.-H. Jung, H.-S. Kim, M.-H. Ryu, and J.-W. Baek, "Design methodology of bidirectional CLLC resonant converter for high-frequency isolation of DC distribution systems," *IEEE Trans. Power Electron.*, vol. 28, no. 4, pp. 1741–1755, Apr. 2013.

[7] W. Chen, P. Rong, and Z. Lu, "Snubberless bidirectional DC–DC converter with new CLLC resonant tank featuring minimized switching loss," *IEEE Trans. Ind. Electron.*, vol. 57, pp. 3075–3086, Sep. 2010.

[8] S. Kenzelmann, A. Rufer, D. Dujic, F. Canales, and Y. R. de Novaes, "Isolated DC/DC structure based on modular multilevel converter," *IEEE Trans. Power Electron.*, vol. 30, no. 1, pp. 89–98, Jan. 2015.

[9] I. A. Gowaid, G. P. Adam, A. M. Massoud, S. Ahmed, D. Holliday, and B. W. Williams, "Quasi two-level operation of modular multilevel converter for use in a high-power DC transformer with DC fault isolation capability," *IEEE Trans. Power Electron.*, vol. 30, no. 1, pp. 108–123, Jan. 2015.

[10] M. Wang, S. Pan, X. Zha, J. Gong, W. Lin, J. Gao, and Q. Deng, "Hybrid control strategy for an integrated DAB–LLC–DCX DC–DC converter to achieve full-power-range zero-voltage switching," *IEEE Trans. Power Electron.*, vol. 36, no. 12, pp. 14383–14397, Dec. 2021.

[11] G. Deng, Y. Sun, G. Xu, X. Chen, S. Xie, S. Yan, M. Su, and Y. Liao, "ZVS analysis of half bridge LLC-DCX converter considering the influence of resonant parameters and loads," in *Proc. IEEE Energy Convers. Congr. Expo. (ECCE)*, Oct. 2020, pp. 1186–1190.

[12] J. Xu, J. Yang, G. Xu, T. Jiang, M. Su, Y. Sun, H. Wang, and M. Zheng, "PWM modulation and control strategy for LLC-DCX converter to achieve bidirectional power flow in facing with resonant parameters variation," *IEEE Access*, vol. 7, pp. 54693–54704, 2019.

[13] P. Wang, S. Feng, P. Liu, N. Jiang, and X.-P. Zhang, "Nyquist stability analysis and capacitance selection for DC current flow controllers in meshed multi-terminal hvdc grids," *CSEE J. Power Energy Syst.*, vol. 7, no. 1, pp. 114–127, 2021.

[14] M. Tabari and A. Yazdani, "Stability of a DC distribution system for power system integration of plug-in hybrid electric vehicles," *IEEE Trans. Smart Grid*, vol. 5, no. 5, pp. 2564–2573, Sep. 2014.

[15] R. P. Barcelos and D. Dujic, "Direct current transformer impact on the DC power distribution networks," *IEEE Trans. Smart Grid*, vol. 13, no. 4, pp. 2547–2556, Jul. 2022.

[16] J. M. Burdio, L. A. Barragan, F. Monterde, D. Navarro, and J. Acero, "Asymmetrical voltage-cancellation control for full-bridge series resonant inverters," *IEEE Trans. Power Electron.*, vol. 19, no. 2, pp. 461–469, Mar. 2004.

[17] Y. Cao, M. Ngo, R. Burgos, A. Ismail, and D. Dong, "Switching transition analysis and optimization for bidirectional CLLC resonant DC transformer," *IEEE Trans. Power Electron.*, vol. 37, no. 4, pp. 3786–3800, Apr. 2022.

[18] X. Yu and P. Yeaman, "A new high efficiency isolated bi-directional DC–DC converter for DC-bus and battery-bank interface," in *Proc. IEEE Appl. Power Electron. Conf. Expo. (APEC)*, Mar. 2014, pp. 879–883.

[19] K. Tan, R. Yu, S. Guo, and A. Q. Huang, "Optimal design methodology of bidirectional LLC resonant DC/DC converter for solid state transformer application," in *Proc. 40th Annu. Conf. IEEE Ind. Electron. Soc. (IECON)*, Oct. 2014, pp. 1657–1664.

[20] J. Zhang, J. Liu, J. Yang, N. Zhao, Y. Wang, and T. Q. Zheng, "An LLC-LC type bidirectional control strategy for an LLC resonant converter in power electronic traction transformer," *IEEE Trans. Ind. Electron.*, vol. 65, no. 11, pp. 8595–8604, Nov. 2018.

[21] J. Kucka and D. Dujic, "Smooth power direction transition of a bidirectional LLC resonant converter for DC transformer applications," *IEEE Trans. Power Electron.*, vol. 36, no. 6, pp. 6265–6275, Jun. 2021.

[22] G. Ulissi, U. R. Vemulapati, T. Stiasny, and D. Dujic, "High-frequency operation of series-connected IGCTs for resonant converters," *IEEE Trans. Power Electron.*, vol. 37, no. 5, pp. 5664–5674, May 2022.

[23] D. Dujic, G. K. Steinke, M. Bellini, M. Rahimo, L. Storasta, and J. K. Steinke, "Characterization of 6.5 kV IGBTs for high-power medium-frequency soft-switched applications," *IEEE Trans. Power Electron.*, vol. 29, no. 2, pp. 906–919, Feb. 2014.

[24] J. Huang, X. Zhang, Z. Shuai, X. Zhang, P. Wang, L. H. Koh, J. Xiao, and X. Tong, "Robust circuit parameters design for the CLLC-type DC transformer in the hybrid AC–DC microgrid," *IEEE Trans. Ind. Electron.*, vol. 66, no. 3, pp. 1906–1918, May 2019.

[25] N. Djekanovic and D. Dujic, "Copper pipes as medium frequency transformer windings," *IEEE Access*, vol. 10, pp. 109431–109445, 2022.

[26] N. Djekanovic, M. Luo, and D. Dujic, "Integrated simulation approach to loss calculations of power converter systems," in *Proc. PCIM Eur. Digit. Days Int. Exhib. Conf. Power Electron., Intell. Motion, Renew. Energy Manag.*, 2020, pp. 1–8.

[27] M. Mogorovic and D. Dujic, "100 kW, 10 kHz medium-frequency transformer design optimization and experimental verification," *IEEE Trans. Power Electron.*, vol. 34, no. 2, pp. 1696–1708, Feb. 2019.

[28] N. Djekanovic, M. Luo, and D. Dujic, "Modeling and integrating losses of magnetic components into time-domain electric circuit simulations," in *Proc. IEEE 9th Int. Power Electron. Motion Control Conf. (IPEMC-ECCE Asia)*, Nov. 2020, pp. 1055–1062.

[29] J. Sun, L. Yuan, Q. Gu, and Z. Zhao, "Startup strategy with constant peak transformer current for solid-state transformer in distribution network," *IEEE Trans. Ind. Appl.*, vol. 55, no. 2, pp. 1740–1751, Mar. 2019.

[30] Q. Chen, J. Wang, Y. Ji, and S. Liang, "Soft starting strategy of bidirectional LLC resonant DC–DC transformer based on phase-shift control," in *Proc. 9th IEEE Conf. Ind. Electron. Appl.*, Jun. 2014, pp. 318–322.

[31] B. Lu, W. Liu, Y. Liang, F. Lee, and J. van Wyk, "Optimal design methodology for LLC resonant converter," in *Proc. 21st Annu. IEEE Appl. Power Electron. Conf. Expo. (APEC)*, Mar. 2006, p. 6.

RENAN PILLON BARCELOS (Graduate Student Member, IEEE) received the B.S. degree in electrical engineering from the Federal University of Santa Maria (UFSM), Brazil, in 2018, and the M.Sc. degree from the Federal University of Santa Catarina (UFSC), Brazil, in 2020. Since 2021, he has been a Doctoral Assistant with the Power Electronics Laboratory, École Polytechnique Fédérale de Lausanne (EPFL), Switzerland. His research interests include modeling, design, system identification, and stability in domain of DC power distribution networks with DC transformers.

JAKUB KUCKA (Member, IEEE) received the bachelor's and master's degrees from Czech Technical University, Prague, Czech Republic, in 2012 and 2014, respectively, and the Dr.-Ing. (Ph.D.) degree from Leibniz University Hannover, Hanover, Germany, in 2019, all in electrical engineering. From 2014 to 2019, he was a Research Associate with the Institute for Drive Systems and Power Electronics, Leibniz University Hannover. After, he was a Postdoctoral Researcher with the Power Electronics Laboratory, EPFL, Lausanne, Switzerland, until November 2021. Since then, he has been with Large Drives Applications, Siemens AG, Erlangen, Germany. He has authored more than 30 scientific publications, two tutorials, and filed five patent applications. His research interests include modular multilevel converters, converter control and design, and resonant converter topologies suitable for high-power DC applications. He was a recipient of EPE Outstanding Young Member Award, in 2020, and SEMIKRON Young Engineer Award, in 2021.

DRAZEN DUJIC (Senior Member, IEEE) received the Dipl.-Ing. and M.Sc. degrees from the University of Novi Sad, Novi Sad, Serbia, in 2002 and 2005, respectively, and the Ph.D. degree from Liverpool John Moores University, Liverpool, U.K., in 2008, all in electrical engineering.

From 2002 to 2006, he was with the Department of Electrical Engineering, University of Novi Sad, as a Research Assistant. From 2006 to 2009, he was with Liverpool John Moores University, as a Research Associate. From 2009 to 2013, he was with the ABB Corporate Research Centre, Switzerland, as the Principal Scientist, working on the power electronics projects spanning the range from low-voltage/power SMPS in below kilowatt range to medium voltage high-power converters in a megawatt range. From 2010 to 2011, he was a member of a project team responsible for the development of the world's first power electronic traction transformer successfully commissioned on the locomotive. From 2013 to 2014, he was with ABB Medium Voltage Drives, Turgi, Switzerland, as the Research and Development Platform Manager, responsible for ABB's largest IGCT-based medium voltage drive ACS6000. He is currently with the École Polytechnique Fédérale de Lausanne (EPFL), Lausanne, Switzerland, as an Associate Professor and the Director of the Power Electronics Laboratory. He has authored or coauthored more than 200 scientific publications and has filed 20 patents. His current research interests include the areas of design and control of advanced high-power electronics systems for medium voltage applications.

Dr. Dujic has received the First Prize Paper Award from the Electric Machines Committee of the IEEE Industrial Electronics Society, in 2007. In 2014, he has received the Isao Takahashi Power Electronics Award for Outstanding Achievement in Power Electronics, and in 2018, the EPE Outstanding Service Award from the European Power Electronics and Drives Association. He is an Associate Editor of the IEEE Transactions on Industrial Electronics, the IEEE Transactions on Power Electronics, and the *IET Electric Power Applications*.

● ● ●